THE SEASONDE HIGH-FREQUENCY RADAR SYSTEM FOR SURFACE CURRENT MEASUREMENTS

By

Donald O. Hodgins

Seaconsult Marine Research Ltd.
8805 Osler Street, Vancouver, B.C. V6P 4G1

ABSTRACT

SeaSonde is a new generation of HF radar system for remote sensing ocean surface currents. Advantages include an FMCW signal format giving improved range at lower transmit power and better current accuracy, improved compact loopstick antenna systems, solid state RF electronics for compact, reliable operation, data acquisition controlled by personal computers, and powerful data display and processing options with a user-friendly graphic interface. Intercomparison of currents measured with the new SeaSonde with drifter data have shown the SeaSonde speeds to be unbiased, with mean absolute speed differences of 4 to 5 cm/s. Trajectories calculated from the SeaSonde surface currents showed good agreement with the drifters, reproducing tidally induced loops and eddies in the flow. Separation scales of the predicted and measured trajectories were typically 9 ± 2 km after 48 h. The SeaSonde currents provide reliable, real-time maps of surface currents, and form an important new resource for understanding ocean circulation.

1. INTRODUCTION

Over continental shelves the surface circulation is notably variable, responding to tides, winds, density variations and low-frequency shelf waves. Much of this variability is not predictable with present numerical models or from available oceanographic data, and as a result pollutant dispersion, or oilspill projections tend to be inaccurate. A good understanding of circulation features requires a spatial current mapping technique wherein currents are measured simultaneously over the area of interest. Such data provide new possibilities for spatial analysis, and they are amenable to conventional time-series analysis, or assimilation into circulation models such as GF8/9 (Stronach, 1992). At this time, HF radar remote sensing techniques provide the only practical means of obtaining surface current maps that cover enough of the shelf seas to give a comprehensive picture of circulation.

2. BACKGROUND TO HF RADAR

Over 35 years ago Crombie (1955) first explained the strong, distinctive symmetric peaks observed in HF sea-echo Doppler spectra in terms of Bragg scatter from surface waves. Crombie (1972) also suggested the use of these peaks to deduce surface currents, and devised an experiment utilizing a direction-finding two-element antenna pair to sense the magnitude and direction of the Gulf Stream flow off Cape Kennedy, Florida. The radial speed was related to bearing direction through the phase differences between the two antenna elements at each Doppler spectral frequency in the Bragg peak echoes.

In the absence of currents, the Bragg mechanism produces sea echo peaks that appear at Doppler positions proportional to the phase speed of waves whose lengths are exactly half the radar wavelength. For a given radar frequency, usually between 6 to 26 MHz, the wave length is known, and the reference position of these peaks can be precisely calculated. Any underlying radial component of current near the surface at the point of scatter will impart an additional shift from the reference position that is converted to speed through the Doppler relation.

Proceedings 3rd ASEAN Science & Technology Week, September 17-24, 1992, Singapore.

The surface waves producing the echo are essentially tracers for the water current, analogous to turbulent scatterers in water that produce the return signal sensed by subsurface acoustic Doppler current profilers. Upper HF radar frequencies are selected since they scatter from short waves with periods of about 3 s; there is almost always some energy in these waves, even under the calmest conditions. The HF radars accurately measure horizontal currents in the uppermost layers, where other instruments such as current meters and acoustic doppler profilers become inoperable. For this reason, the HF measured currents are ideal for oil or pollutant dispersion calculations at the water surface.

The Bragg scatter mechanism yields information on current variations radial to the radar (i.e. pointing away from or toward the radar). Thus, two sites must view a point on the water in order to produce an unambiguous estimate of the total horizontal current vector. HF radar signal formats (pulse or linearly swept frequency) employ time delay to isolate the return from a annular segments of ocean at different radial distances from the coast (Fig. 1a). Two methods are generally employed to isolate the scattering patch in bearing: beam forming and direction finding (DF) methods. HF current-sensing systems that employ DF methods have become known as CODARs (Lipa and Barrick, 1973), and feature compact antenna systems with three or four elements. The newest version is called the SeaSonde.

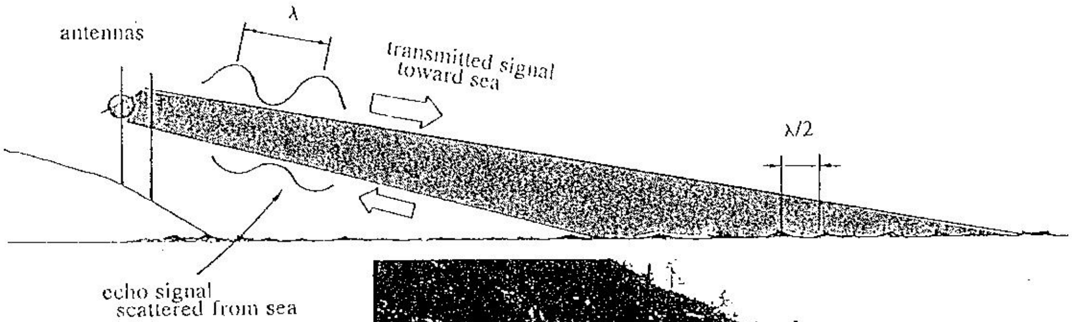

(a)

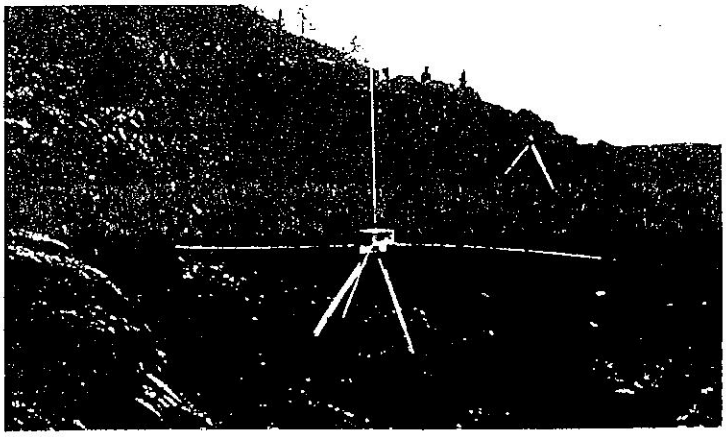

(b)

Figure 1

SeaSonde principles (a) and photograph (b) of the antennas

3. SEASONDE FEATURES AND MEASUREMENT PROPERTIES

3.1 Features

SeaSonde is a highly portable 12.5 MHz radar system for mapping currents over a broad expanse of ocean. It utilizes two or more radar sites separated by 30 to 50 km along the coast. Each radar consists of the transmit/receive hardware and a Macintosh computer for data acquisition and control. Radial current components are computed at each remote site and transmitted by landline, UHF radio, or satellite data link, to a central-site computer (PC DOS system running windows 3.0) where they are combined into the total current map. Each radar has a range exceeding 60 km, with a range ring spacing of 2.56 km; thus, coverage usually exceeds 2,000 km^2.

SeaSonde uses compact, cross-loopstick antennas for the receiver and a single monopole whip for transmit. This results in light, portable antennas, each of which can be mounted on a single guyed post, or surveyors tripod (Fig. 1b). The installation time is less than 1 hour from arrival on site to start of data reception. The small antenna footprint means that virtually any kind of terrain is accessible, and security is seldom a problem. Transmit power is less than 100 W, making licensing problems minimal. Power consumption is low, less than 1,500 W at each radar site. During a deployment in August 1991, one unit was run for over 20 days on a single 1,500 W portable generator. The RF electronics and computer were housed in a 2-man tent.

The central site computer, through which the user accesses the data, has a full windows environment for data manipulation, display, plotting and archiving. All results are fully geo-referenced using digitized coastlines, and the currents are calculated on Cartesian grids superimposed on the radar coverage area. Grid set-up parameters are readily changed to examine the effects of altering the spacing and orientation. Data can be acquired, blended and plotted automatically, or the user can override the autoprocessing function and manually examine data. The central site software takes care of communications, and is written to allow more than two remote radar sites to send in radial data.

Codar principles for measuring surface currents are summarized in Hodgins (1991) and Hardy et al. (1989), and are described in detail in Lipa and Barrick (1983). In the new SeaSondes an FMCW (frequency-modulated continuous wave) signal format is used, centered at a frequency of 12.5 MHz. The voltages from each receive antenna are Fourier transformed using a 512-point FFT. The spectral resolution is 0.00391 Hz, which for the radar frequency of 12.5 MHz is equivalent to a Doppler velocity resolution of approximately 3.3 cm/s. A running spectral average is then formed from 14 consecutive sample spectra, and the averaged Doppler spectra in each range ring are used for the extraction of radial velocities. The radial velocities represent a 1-h time average of the actual flow field.

SeaSonde advantages include:

- high portability and rapid deployment;
- few siting restrictions;
- ranges exceeding 60 km, coverage areas > 2,000 km^2;
- low transmit power and minimal licensing requirements;
- low initial cost and low field operating costs;
- proven algorithms for current extraction;
- real-time total current map production;
- user friendly radar site software for monitoring and control;
- user friendly, comprehensive central software for data analysis;
- automated data acquisition for long-term monitoring.

3.2 Surface current measurements

In August 1991 the new SeaSonde was deployed in a wilderness area on the Canadian west coast to monitor strong tidal surface currents over a 21-day period. Four days of near-surface drogued drifter data were collected for comparison with the radar-measured currents. Current meter data were also collected in 1990 in the same area. The rugged, inaccessible terrain provided only two possible sites at which to locate the radar units, located 16.8 km along the baseline as shown in Fig. 2.

Radial velocities at each radar were extracted from the sea-echo spectra using the least-squares method described by Lipa and Barrick (1983). Total current vectors were calculated by combining the radial data from each radar site on a 1 km by 1 km Cartesian grid (EW-NS orientation) within the coverage area. The coverage area was divided into area cells, and all radial velocities from both radars falling into a given cell were interpreted to give a total current velocity. The circular area cells have been centered on each Cartesian grid point, defined by a blending radius R_b. The total current speed and direction were found by least-squares fitting to the radial components following the algorithm described in Lipa and Barrick (1983). The optimum blending radius was found to be R_b=5 km (Hodgins and Hardy, 1992). An example of one pair of radial currents maps, and the corresponding total vector field is shown in Fig. 3.

3.3 Drifter and current meter data

Sea Rover drifting buoys were deployed in or near the radar coverage area between August 21 and 24, 1991. Each drifter was fitted with a 5-m long holey sock drogue and eight independent drift tracks were measured, ranging in duration from 17.5 to 48 h. The time between position fixes was 30 minutes. The Sea Rover buoys use Loran C for positioning, which in Queen Charlotte Sound is believed to be accurate to no better than ±50 m (pers. comm., W. Crawford, Institute of Ocean Sciences, 1992). The corresponding error in the velocity components is ±4 cm/s. Winds during this period were moderate, at 10 to 20 knots steady from the northwest, with brief periods of speeds of 5 to 10 knots.

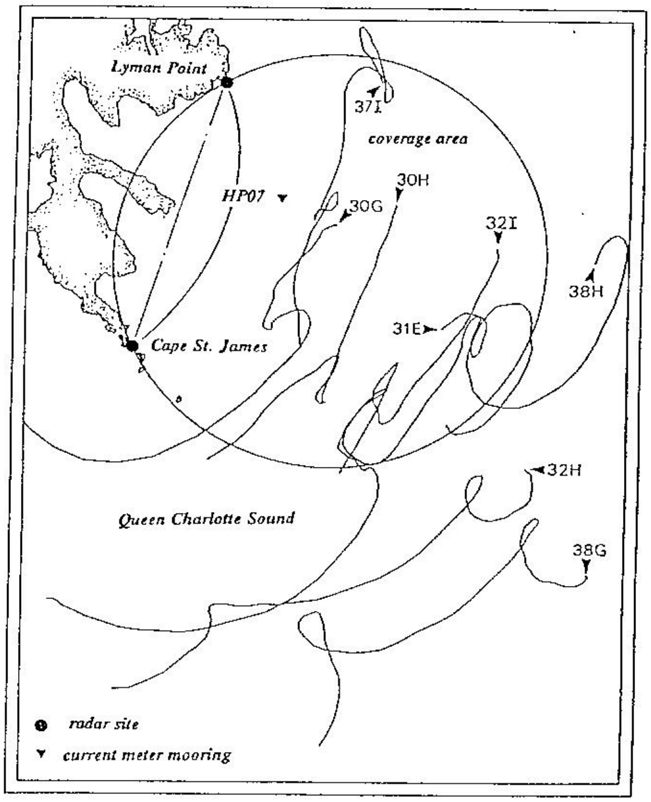

Figure 2 Map of SeaSonde coverage area in Queen Charlotte Sound and drifter tracks.

In 1990-91 current meter data were also obtained at the mooring location HP07 (Fig. 2) at 100 m depth. The time-series for the summer months of July and August (similar stratification conditions and tidal amplitudes to the SeaSonde period) were used to calculate the tidal harmonic constants. The tidal current for August 1991 was then reconstituted using these harmonic constants and compared with the tidal component of the SeaSonde data.

4. COMPARISON OF SEASONDE AND DRIFTER CURRENTS

4.1 Eulerian statistics

Radial current speeds are compared with the equivalent drifter component speeds for three trajectories (I37, H30, and H38) in Fig. 4. Two of the trajectories are centered in the coverage area, and one (H38) lies mainly outside the area. The radial current at each drifter position has been calculated from the SeaSonde data using a 4-point bilinear interpolation in range and bearing, weighted inversely by the variance of each radial speed. Generally, the data from each site plot on opposite sides of zero. The correlation of radial speeds is high for all drifters; however, the scatter is slightly greater at H38 than at closer ranges. The scatter is typical of comparisons of averaged currents with results from punctual drifter data.

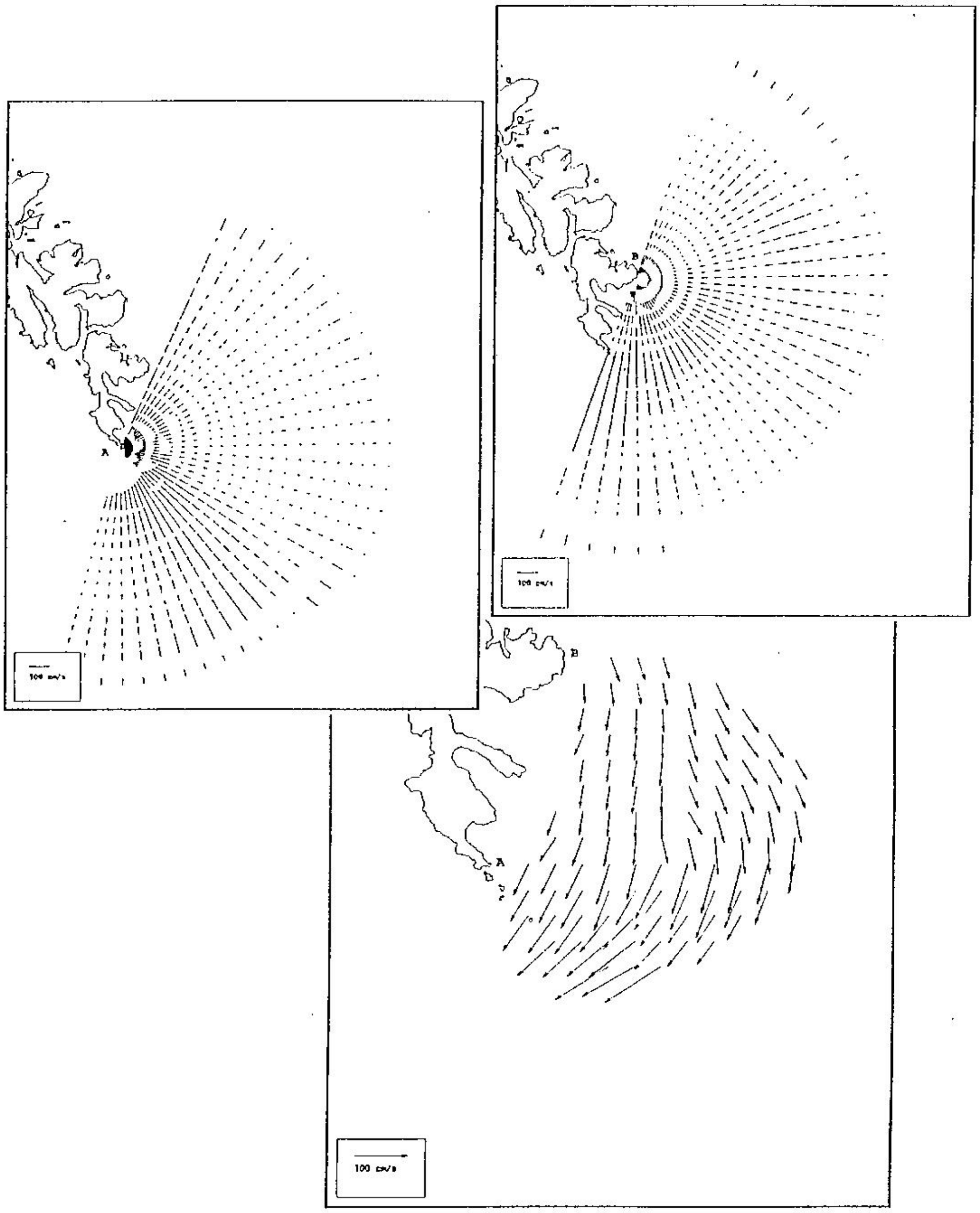

Surface current field: Cape St James, Queen Charlotte Islands, 01:33 GMT, August 14, 1991. Radar sites were located at Cape St James (A) and Lyman Point (B).

Figure 3 Radial current fields from two SeaSonde sites in Queen Charlotte Sound (upper panels), and total surface current (lower panel).

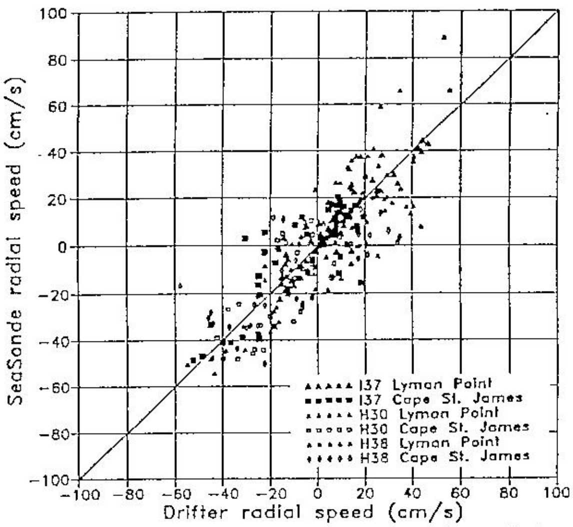

Figure 4 Correlation of SeaSonde radial currents with drifter observations.

Surface currents components, combined with a radius $R_b = 5$ km, are compared with the drifter current vectors for tracks I37 and H30 in Fig. 5. These tracks were chosen for their central position in the coverage area. Speeds ranged from less than 5 cm/s to over 80 cm/s, and the SeaSonde shows a high correlation with the drifter data. The average absolute difference in total current speed for these trajectories (104 observations) is 7.8 cm/s with a standard deviation of 6.7 cm/s. Assuming that about ± 4 cm/s of this difference is accounted for by the error in the drifter velocity, it appears that the radar and drifter differ by about an equivalent amount. The drifter speeds are calculated from punctual data, and thus do not provide an equivalent measure to the 1-h average of the SeaSonde. Moreover, the drifters integrate about 5 m of the surface shear, and differ slightly from the SeaSonde measurement. Thus, the additional difference of ± 3 to ± 4 cm/s likely arises from the real difference between the surface current and the 5-m drogued drift current, and from error in the radar measurement.

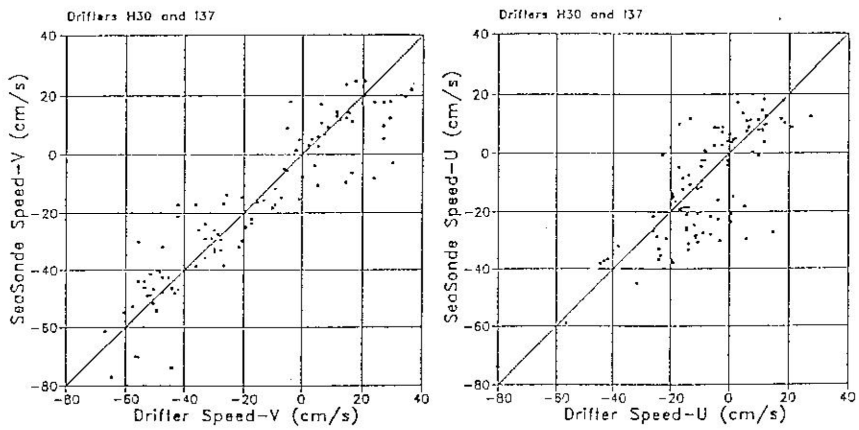

Figure 5 Correlation of SeaSonde total current components with drifter currents.

4.2 Lagrangian Comparison

The currents measured with the radar have been used to calculate a set of trajectories initialized at the time and location of the beginning of the measured drift tracks. The predicted trajectories have been calculated from the relation

$$\mathbf{X}(t) = \int_0^t \mathbf{U}_s(x,t)\, dt \qquad (1)$$

where $\mathbf{X}$ is the position vector and $\mathbf{U}_s$ is the surface current vector derived from the SeaSonde radial currents with $R_b = 5$ km. A two-step predictor-corrector procedure, applied at each integration subinterval Δt, was used to integrate (1) for each 30 min time increment, i.e.

$$X(N\Delta t) = \sum_{n=0}^{N} <_l U_s> \cdot \Delta t + X(0\Delta t), \quad l=1,2 \tag{2}$$

where $<_l U_s> = (U^{n+1} + U^n)/2$, with $U^{n+1} = U^n$ for $l=1$ and l is the iteration number.

Representative comparisons of predicted and measured trajectories are shown in Fig. 6. The trajectories generally exhibit good agreement, where many of the tidally induced eddy-like features found in the drifter tracks are reproduced by the SeaSonde predictions. On balance, the total displacement of the SeaSonde tracks is slightly greater than the drifters, consistent with a stronger currents right at the sea surface than integrated over the drogue depth.

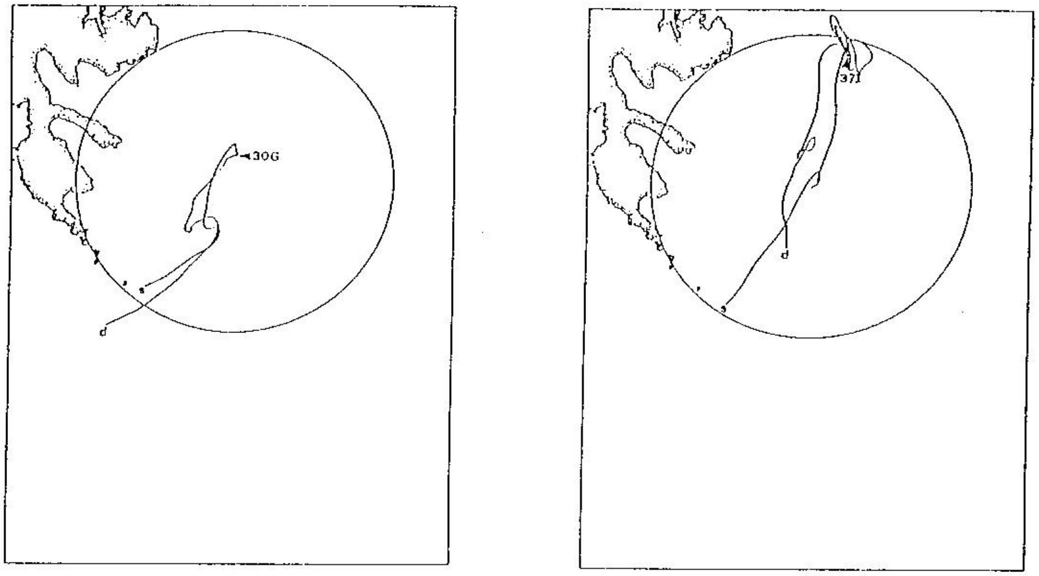

Figure 6 Comparison of predicted (s) and measured (d) drift for trajectories G30 (left) and I37 (right).

5. COMPARISON OF SEASONDE AND CURRENT METER DATA

Currents in Queen Charlotte Sound contain both barotropic and baroclinic components, produced by density variations and tidal rectification. However, the principal tidal components are expected to be mainly barotropic. The tidal portion of the SeaSonde signal is compared with the equivalent signal from the current meter in Fig. 7. The mean component has been removed since it is depth-dependent. Phase agreement between the two signals is excellent. Amplitude variations in both the u- and v-components are in close agreement for the first 12 days of the comparison; thereafter, the SeaSonde data exhibit slightly more energy than the current meter, particularly on the flood phase of the tide.

The close correspondence of the SeaSonde tidal signal with the current meter provides good confidence in the accuracy of the HF methods.

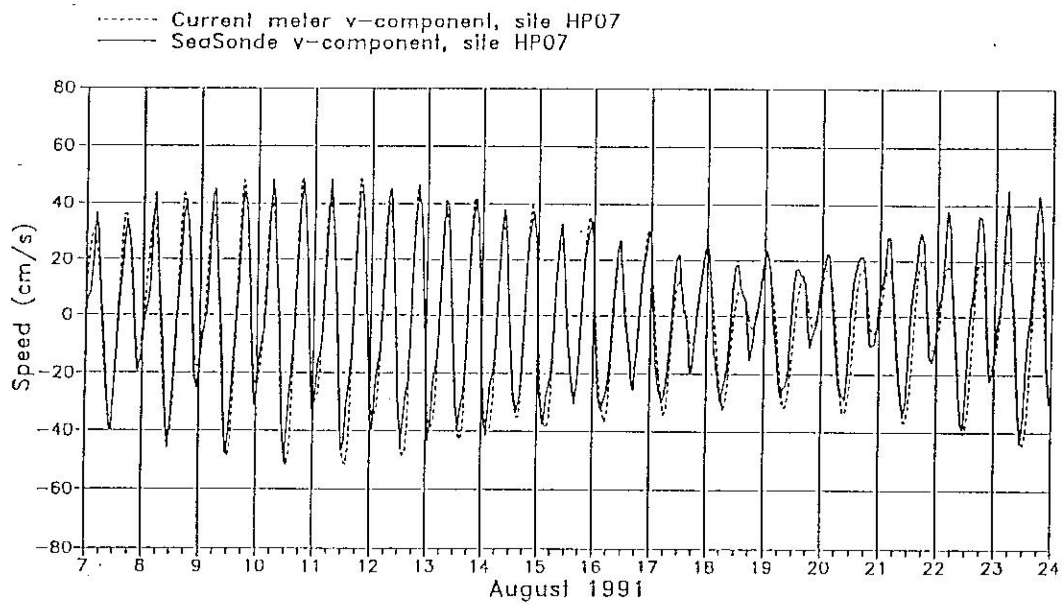

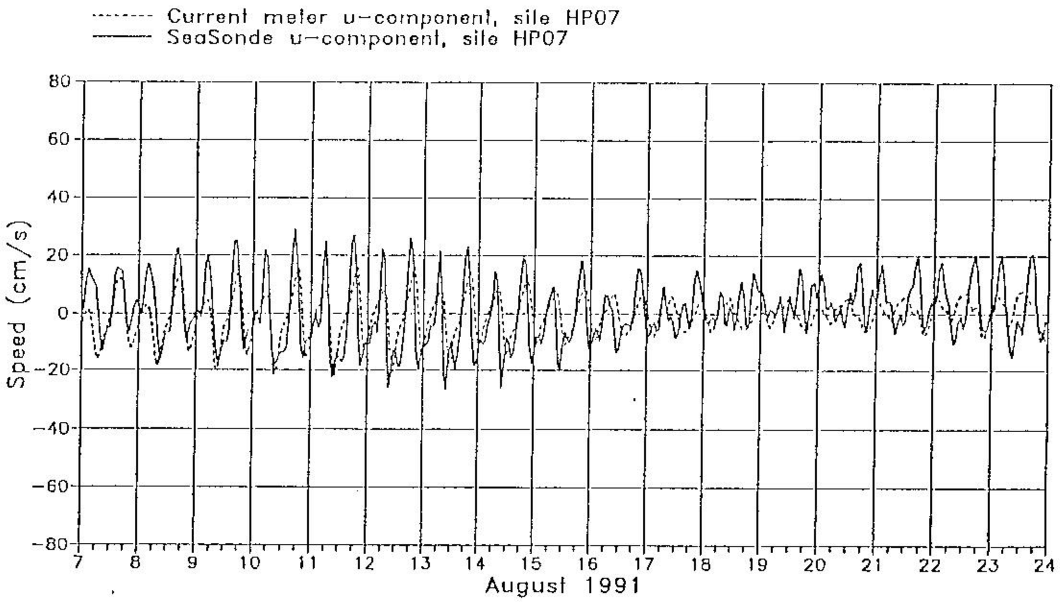

Figure 7 Comparison of SeaSonde tidal current components with current meter observations.

6. CONCLUSIONS

Comparison of both radial and combined total current speeds and directions with individual drifter tracks showed a high correlation. In the coverage area the mean absolute difference between drifter currents and SeaSonde currents was about 7.8 cm/s with a standard deviation of 6.7 cm/s for currents ranging up to 80 cm/s. The SeaSonde measurements were essentially unbiased (mean difference of 0.25 cm/s and standard deviations of 10.3 cm/s). The drifter speed error is estimated to be about ± 4 cm/s based on the positional uncertainty of Loran-C in the study area; thus, the mean difference between drifter and SeaSonde currents is approximately 4 to 5 cm/s.

A Lagrangian comparison showed that predicted drift from the SeaSonde data reproduced the tidally-induced eddies and loops exhibited by the drifters, as well as the overall drift patterns. Based on linear regression of the separation distance with time for the three longest tracks, representative separation scales are 7 ± 1.5 and 9 ± 2 km for drift times of 36 and 48 h for targets within the coverage area of the radars. The excellent agreement of the tidal portion of the signal, the repeatability of flow features in the current maps for similar tidal phases, and the comparisons with drifter data discussed previously, show that the HF radar sensing technique provides accurate maps of the surface circulation. Downwelling and upwelling features are clearly present. SeaSonde presents new opportunities to measure and understand ocean dynamics on a regional scale.

7. ACKNOWLEDGEMENTS

The deployment of the SeaSonde radar system, and collection of the drifter data for comparison with the surface current measurements, was undertaken as part of PERD Project 62142, administered by Fisheries & Oceans Canada (Dr. D. Masson). Funding was also provided by the Emergencies Science Division of Environment Canada and the Canadian Coast Guard.

8. REFERENCES

Crombie, D.D., 1955. Doppler Spectrum of Sea Echo at 13.56 Mc/s. *Nature*, 175, 681-682.

Crombie, D.D., 1972. Resonant Backscatter from the Sea and its Application to Physical Oceanography. Oceans '72 Conf. Rec., IEEE Publ. No. 72CHO 660-1 OCC, 173-179.

Hardy, J.S., D.S. Dunbar and D.O. Hodgins, 1989. An Evaluation of Methods for Extracting Surface Currents from CODAR Data. Proc. IGARRS '89, 12th Canadian Symposium on Remote Sensing, Vancouver, Canada.

Hodgins, D.O., 1991. New Capabilities in Real-time Oil Spill and Fate Prediction Using HF Radar Remote Sensing. Proc. 14th AMOP Technical Seminar, June 12-14, 1991, Vancouver, Canada.

Hodgins, D.O. and J.S. Hardy, 1992. Surface Current Data from Queen Charlotte Sound, B.C., Intercomparison of SeaSonde and Drifter Current Observations. Prepared for Fisheries & Oceans, Canada, Canadian Coast Guard, and Environment Canada by Seaconsult Marine Research Ltd.

Stronach, J.S., 1992. Applications of Three-dimensional Hydrodynamic Models. Proc. ASEAN 3rd Science & Technology Week-Regional Ocean Dynamics Conference, Singapore, Sept. 17-24, 1992.

Lipa, B.J. and D.E. Barrick, 1983. Least-Squares Methods for the Extraction of Surface Currents From CODAR Crossed-Loop Data: Application at ARSLOE. IEEE *J. Oceanic Eng.*, OE-8(4), 226-253.